magnetochemistry

MDPI

Article

μSR-Study of a 3% $CoFe_2O_4$ Nanoparticle Concentration Ferrofluid

S. I. Vorob'ev [1,*], M. Balasoiu [2,3,*], D. Buzatu [4], V. N. Duginov [2], A. L. Getalov [1], K. I. Gritsaj [2], E. N. Komarov [1], S. A. Kotov [1], C. Stan [4] and G. V. Scherbakov [1]

[1] NRC «Kurchatov Institute»—PNPI, 188300 Gatchina, Leningrad Region, Russia; getalov_al@pnpi.nrcki.ru (A.L.G.); komarov_en@pnpi.nrcki.ru (E.N.K.); kotov_sa@pnpi.nrcki.ru (S.A.K.); vsiloa@pnpi.spb.ru (G.V.S.)
[2] Joint Institute for Nuclear Research, 141980 Dubna, Moscow Region, Russia; duginov@jinr.ru (V.N.D.); gritsaj@jinr.ru (K.I.G.)
[3] Horia Hulubei National Institute of Physics and Nuclear Engineering, 77125 Bucharest, Romania
[4] Department of Physics, University POLITEHNICA of Bucharest, 060042 Bucharest, Romania; danielle_buzatu@yahoo.com (D.B.); cvstan67@gmail.com (C.S.)
* Correspondence: Vorobyev_SI@pnpi.nrcki.ru (S.I.V.); balas@jinr.ru (M.B.); Tel.: +7-813-714-6512 (S.I.V.); +7-496-216-3099 (M.B.)

Abstract: Magnetic fluids based on single-domain magnetic spinel ferrite nanoparticles dispersed in various liquid media are of particular practical and scientific interest. This paper presents a muon spectroscopy study of a ferrofluid based on magnetic nanoparticles of $CoFe_2O_4$ molecules dispersed in water (H_2O) with a nanoparticle concentration of 3%. In this study, it was determined that the structure and magnitude of the magnetization of a ferrofluid depend on the viscosity of the liquid itself. It was shown that, at room temperature (290 K) and under an external magnetic field of 527 G, the observed additional magnetization was ~20 G. In a small fraction of the sample under study (~20%), negative magnetization (diamagnetism) was observed. At low temperatures (~30 K), the sample acted as a paramagnet in a magnetic field. For the first time, the magnetic field inside and in the immediate vicinity of a $CoFe_2O_4$ nanoparticle has been measured experimentally using the μSR method: the value was 1.96 ± 0.44 kG; thus, direct measurement of the magnetization of a nanoscale object was performed.

Keywords: muon; spin precession; magnetoelectric interactions; phase transitions; incommensurate magnetic structure; doped and nanostructured materials

Citation: Vorob'ev, S.I.; Balasoiu, M.; Buzatu, D.; Duginov, V.N.; Getalov, A.L.; Gritsaj, K.I.; Komarov, E.N.; Kotov, S.A.; Stan, C.; Scherbakov, G.V. μSR-Study of a 3% $CoFe_2O_4$ Nanoparticle Concentration Ferrofluid. *Magnetochemistry* **2021**, *7*, 104. https://doi.org/10.3390/magnetochemistry7070104

Academic Editor: Jose Maria Porro

Received: 17 May 2021
Accepted: 12 July 2021
Published: 14 July 2021

1. Introduction

Magnetic nanostructures, such as nanoparticles [1–10] or thin layers [11–14], are of great practical and scientific interest due to their special properties, which are caused by nanoscale effects.

For many decades, ferrofluids (FF)—ultrastable dispersions of single-domain nanomagnetic particles in various liquids, stabilized by different methods—have been continuously studied by scientists and engineers [15].

Ferrofluids have been used in an increasingly diverse spectrum of applications in research and/or development, such as seals, lubricants, adjustable dampers, clutches, inkjet printers, cooling for electronic devices, heat transfer, mass density separation, optics applications, various sensors or biosensors, cell separation, the controlled targeting of drugs with magnetic resonance imaging, hyperthermia, etc., to mention a few [3,5,16].

The developments for novel applications are directly connected with active research on the production of new types of ferrofluids, with particles of different sizes, shapes, compositions, and concentrations [17,18], using innovative synthesis and stabilization methods and compounds, as well as conducting studies on their properties. Currently, liquids based on single-domain magnetic nanoparticles of spinel ferrites, $MeFe_2O_4$ (where Me are Cr, Mg, Fe, Co, and Zn), dispersed in various liquid media are widely studied.

The stability of magnetic fluids is achieved by the use of various surfactants that prevent nanoparticles from sticking together [19–21]. The magnetic fluid in water was stabilized at low concentrations (<5–7%) of nanoparticles. At temperatures below the Curie temperature, each nanoparticle had a magnetic moment close to the total moment of molecules in the particle.

The magnetic properties of ferrofluids have been studied with many methods [22–25], including using quantum magnetometers (SQUID) [26,27], Mössbauer spectroscopy [28,29], and small-angle neutron scattering [30–33].

Among various solid-state nuclear techniques, muon spin research (μSR) is a relatively new technique [34,35]. However, as in all fields of science, in applied muon research new methods and techniques are also being developed, and capabilities of existing methods are continuously being expanded to meet challenges posed by new objects of investigation. The positive-muon rotation technique has proven to be an excellent method for investigating static and dynamic local magnetic fields in condensed matter. Due to its positive charge, the muon usually resides at an interstitial site in a crystal; therefore, these regions are normally inaccessible with other more conventional techniques (magnetic resonance, Mössbauer, etc.). Particular attention has been devoted to magnetic oxides and especially to magnetite [36,37].

The Curie temperature for cobalt ferrite is 793 K, and among the spinel ferrites, $CoFe_2O_4$ has the highest magnetic crystallographic anisotropy constant [38]: about 20 times higher than that of magnetite Fe_3O_4, and equal to 1.84×10^6 erg/cm^3 at T = 300 K for cobaltite ($CoFe_2O_4$) nanoparticles of about 32 nm in size.

The μSR method can be used to help understand magnetic phenomena peculiarities in systems containing nanomagnetic particles by determining local magnetic fields in the sample [39].

2. Materials and Methods

2.1. Materials

For these studies, a ferrofluid sample composed of a 3% volume concentration of magnetic nanoparticles in water, stabilized using sodium dodecyl sulfate, $CH_3(CH_2)_{11}SO_4Na$, with a density ρ = 1.01 g/cm^3, and lauric acid, $C_{11}H_{23}COOH$, with a density ρ = 0.88 g/cm^3, was used as a double surfactant layer.

One milliliter of ferrofluid contained 0.17 g of cobalt ferrite, and for every 1 g of $CoFe_2O_4$ nanoparticles, 0.25 g of surfactant was used.

The investigated sample was synthesized at the Institute of Technical Chemistry, Ural Branch of the Russian Academy of Sciences [18,40,41]. Preliminarily, a double separation of nanoparticles by size was carried out on a Biofuge 15R centrifuge for 60 min at 6000 rpm. The particle size distribution was studied at the Center for Advanced Technologies (Moscow State University, www.nanoscopy.ru) using a LEO 912 AB OMEGA high-resolution transmission electron microscope with an accelerating voltage of 120 kV. The size distribution of nanoparticles was approximated by the lognormal distribution function, and the following parameter values were determined: $D_0 = 7.8 \pm 0.1$ nm, $\sigma = 0.40 \pm 0.01$ nm, with the mathematical expectation value $D_m = D_0 \exp(\sigma^2/2) = 8.5$ nm.

2.2. Muon Spin Rotation (μSR) Method

The sample was studied using the μSR setup [42] installed at the output of the muon channel of the SC-1000 synchrocyclotron of the NRC "Kurchatov Institute", PNPI. The principles of μSR and uses of various relaxation (depolarization) functions of the muon spins to describe the time spectra of the μSR signals are presented in studies which have become references in the field [34,43]. At this facility, we have previously conducted studies of ferrofluids based on Fe_3O_4 [39]. The beam of positively charged muons with an average momentum $p_\mu = 90$ MeV/s and a momentum dispersion $\Delta p_\mu / p_\mu = 0.02$ (FWHM) had a longitudinal polarization $p_\mu = 0.90 \div 0.95$.

The ferrofluid sample, packed in a copper cell 80 mm in diameter and 10 mm in height, was placed in a blowdown cryostat, which made it possible to set the temperature with an accuracy of ~0.1 K in the temperature range 10–290 K. An external magnetic field on the sample, transverse to the direction of the muon spin, was created by Helmholtz coils with a stability of ~10^{-3}. The uniformity of the magnetic field in the central region of the magnetic system was no worse than 10^{-4}. The degree of uniformity of the magnetic field was measured both by the standard method using Hall sensors and by the rate of attenuation of the polarization precession in a copper sample with a size of Ø 40 × 5 mm ($\lambda = 0.0053 \pm 0.0031$ μs^{-1}); such uniformity of the field is acceptable for conducting μSR experiments. The Earth's magnetic field and external scattered magnetic fields were compensated for by additional Helmholtz coils to a level of ~0.05 G.

The time spectra of the positrons from the muons' decay were measured simultaneously in two ranges (0 ÷ 10 μs and 0 ÷ 1.1 μs) with channel widths of 4.9 and 0.8 ns/channel, respectively.

The measurement procedure consisted of cooling the sample in a zero external magnetic field (ZFC) to a temperature of 25 K. After that, a magnetic field of 527 G, transverse to the magnetic moment of the muon, was switched on, and ZFC measurements were recorded as the sample was heated to room temperature (290 K). Then, the sample was again cooled to a temperature of 30 K in the same transverse magnetic field of 527 G, and FC measurements were performed.

The experimental data (time spectra) were approximated using the function:

$$N(t) = N_0 \exp(-t/\tau_\mu)[1 + a_s \cdot G_s(t) + a_b \cdot G_b(t)] + B \quad (1)$$

where N_0 is a normalization constant; τ_μ is the muon lifetime (2.197 μs); B is the background of random coincidences, determined by the form of the time spectrum in the part before the beginning of the decay spectrum, t_0; and a_s and $G_s(t)$ are the asymmetry and relaxation function of the observed muon component of the muon spin precession in the sample, respectively. The term $a_b \cdot G_b(t)$ corresponds to the contribution of the constructive background to the observed asymmetry. The constructive background itself is mainly associated with the decay of muons stopped in the copper walls of the container with ferrofluid, and its contribution can be described as follows:

$$a_b \cdot G_b(t) = a_b \cdot \cos(2\pi \cdot F_b \cdot t) \cdot \exp(-\lambda_b \cdot t) \quad (2)$$

The parameters F_b and λ_b, the precession frequency and relaxation rate, respectively, are determined from the processing of the time spectrum measured on a copper sample. The a_b parameter was obtained from the joint processing of two spectra measured on the ferrofluid sample in an external magnetic field ($H \neq 0$) and in a zero magnetic field ($H = 0$):

$$a_s \cdot G_s(t) = a_H \cdot \cos(2\pi \cdot F_H \cdot t) \cdot \exp(-\lambda_H \cdot t) + a_L \cdot \cos(2\pi \cdot F_L \cdot t) \cdot \exp(-\lambda_L \cdot t) \quad \text{for } H \neq 0 \quad (3)$$

$$a_s \cdot G_s(t) = a_1 \cdot \exp(-\lambda_H \cdot t) + a_2 \cdot \exp(-\lambda_L \cdot t) \quad \text{for } H = 0 \quad (4)$$

In this case, the following requirement is imposed:

$$a_1 + a_2 = a_H + a_L \quad (5)$$

The amplitude a_2 of a weakly damped exponent is chosen as a_b.

The indices (H, L) on the parameters (a, λ) correspond to the observed frequencies of the precession of the muon spin F_H and F_L, where $F_H > F_{Cu} > F_L$. The value F_{Cu} corresponds to the rotation frequency of the muon spin in the pure copper sample.

Using the relaxation function (Equation (1)), and taking into account Equations (2) and (3), made it possible to accurately describe the experimental data of FC and ZFC measurements in a wide range of sample temperatures.

In the temperature range of 26–100 K, the time spectra obtained in ZFC measurements are fairly well described using the following single-frequency relaxation function:

$$a_s \cdot G_s(t) = a_H \cdot \cos(2\pi \cdot F_H \cdot t) \exp(-\lambda_H \cdot t) \quad (6)$$

3. Results and Discussion

3.1. Zero Field Measurements

Even in the absence of an external magnetic field, μ^+ will precess around the internal dipolar field. At a sample temperature of 290 K, two measurements were performed in a zero external magnetic field. One was performed before turning on the external field (round light points), as at T = 41 K, and the second measurement was carried out immediately after turning on the magnetic field with a value of H = 527 G. In both measurements, the relaxation functions did not differ from each other within the error limits.

Figure 1 displays the behavior of the relaxation function $G(t)$ at sample temperatures of 290 K and 41 K in a zero external magnetic field. This indicated that the external magnetic field did not lead to the spatial displacement of nanoparticles.

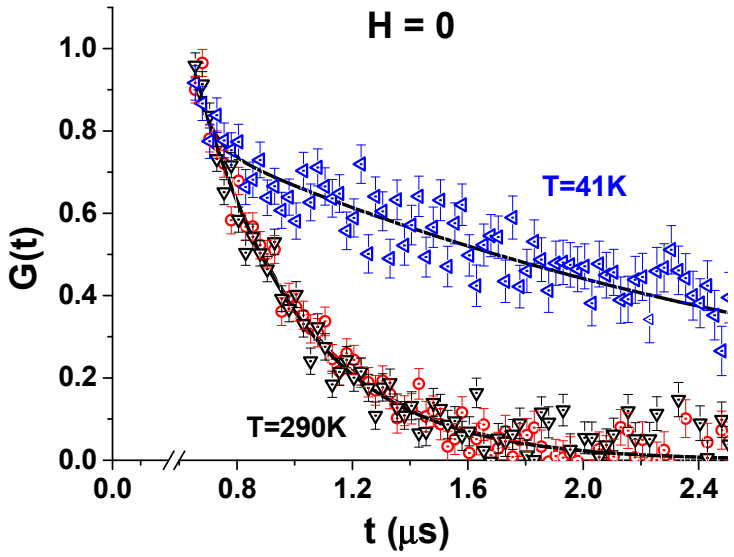

Figure 1. Relaxation function $G(t)$ in a magnetic field H = 0 at T = 41 K (blue triangles) and T = 290 K (light red dots and squares).

The relaxation function at a temperature of 41 K had two components, which sharply differed in terms of the decay rates λ_1 = 0.41 ± 0.02 μs^{-1} and λ_2 = 23 ± 11 μs^{-1}. The rapidly decaying component was apparently associated with the presence of muon stops in the near zone of the scattered fields of nanoparticles, where the inhomogeneity of the magnetic field was high. The separation of the sample volume into near and far zones occurred only at low temperatures when the rotation or oscillation of nanoparticles stopped. At a temperature of 290 K, the entire sample volume was homogeneous in terms of the relaxation rate. This behavior of the relaxation functions was associated with the presence of major anisotropy of the magnetic properties of the nanoparticle itself.

3.2. The Field Scan at the Room Temperature

Further, the sample was measured at room temperature for magnetic field values in the range of up to ~600 G. Figures 2–4 demonstrate the behavior of frequencies, decomposition

rates, and populations as a function of the external magnetic field at the sample temperature of 290 K.

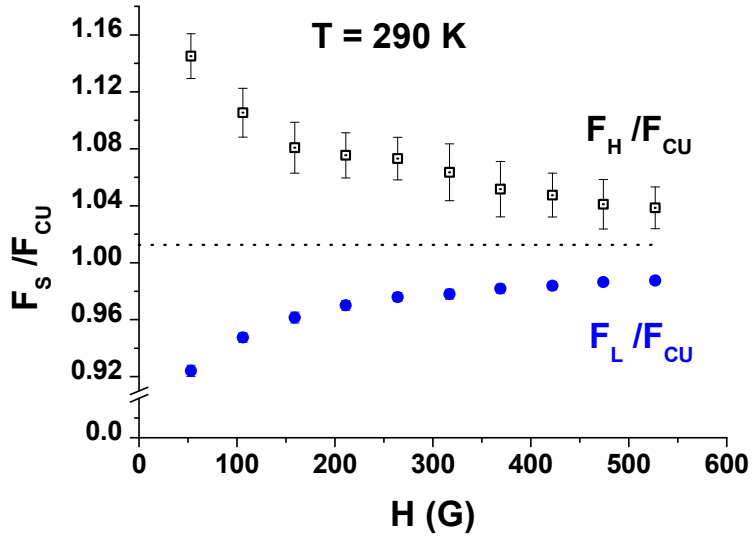

Figure 2. Dependence of the precession frequencies of the muon spin $F_s(s = H, L)$ in the sample on the external magnetic field at a temperature of 290 K (F_H—light points; F_L—dark blue points).

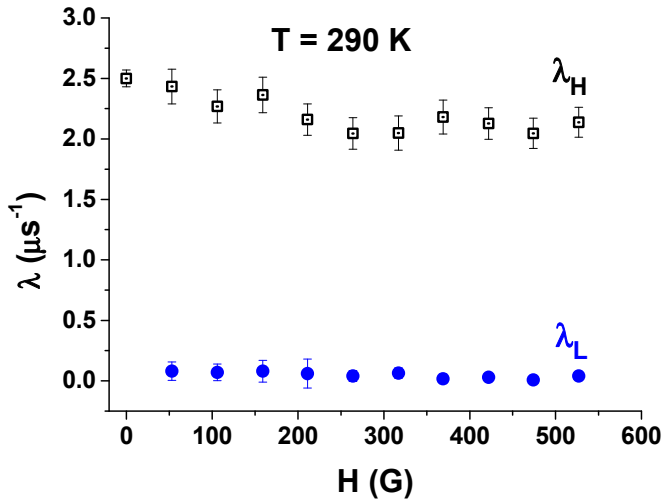

Figure 3. Dependence of the muon relaxation rates on the magnitude of the external magnetic field at a temperature of 290 K (λ_H—light squares; λ_L—dark blue points).

For all external magnetic fields in the range of 50–527 G, the sample under study exhibited muon spin precession at two frequencies, F_H and F_L, in the order $F_H > F_{Cu} > F_L$ (Figure 2). The value F_{Cu} corresponds to the rotation frequency of the muon spin in the pure copper sample.

Additional magnetization was observed in 80% of the sample volume (Figure 4), which, at room temperature (~300 K), corresponded to an additional $\Delta H = 20 \pm 1$ G when the external magnetic field was more than 300 G (Figure 2). In addition, there was a much less noticeable diamagnetic contribution $\Delta H = 6.7 \pm 0.2$ G in 20% of the sample volume (Figures 2 and 4). The relaxation rates λ_H and λ_L, as well as the populations a_H and a_L, practically do not depend on the value of the external magnetic field (Figures 3 and 4). The values of λ_L in Figure 3 are in the range of 0.09–0.12.

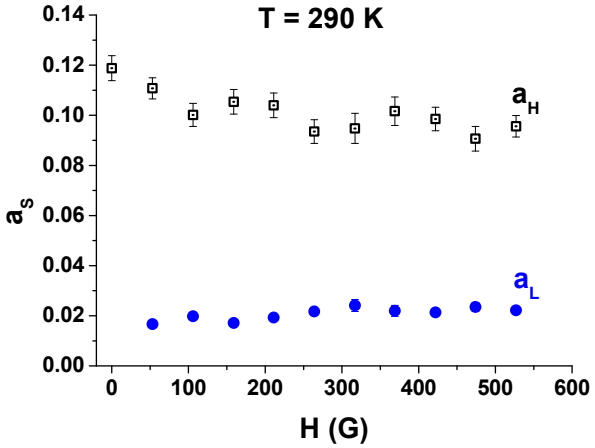

Figure 4. Dependence of the amplitudes of the muon spin precession (populations) on the external magnetic field at a temperature of 290 K (a_H—light points; a_L—dark blue points).

3.3. FC and ZFC Measurements

The behavior of systems with nanoparticles depends on the conditions in which they were cooled. At the FC procedure, the sample is cooled in the magnetic field, whereas the ZFC sample is cooled first in the absence of magnetic field and then the magnetic field is switched on.

Figures 5–8 present the results of processing the time spectra measured on a ferrofluid sample in an external magnetic field H = 527 G in the sample temperature range of 26 K to 290 K. In the FC measurement mode, two muon spin precession frequencies, F_H and F_L, were observed over the entire temperature range (Figure 5).

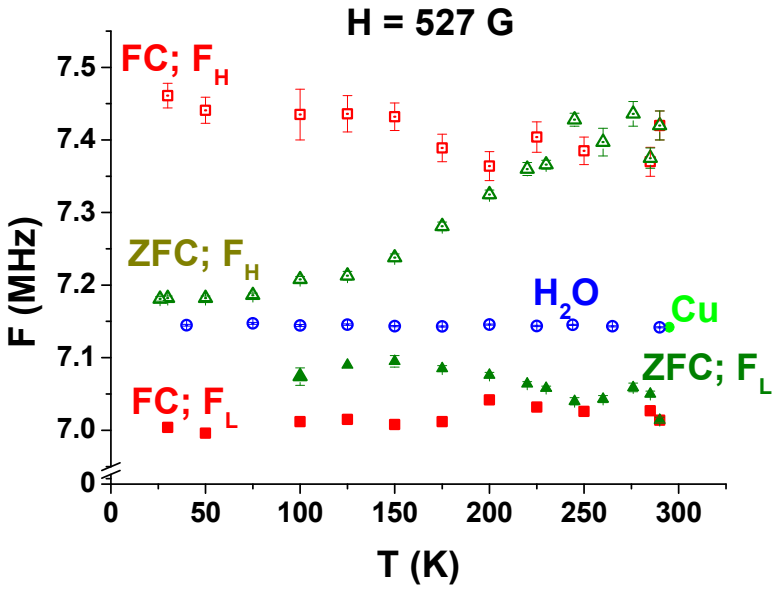

Figure 5. Temperature dependence of the muon spin precession frequencies in a magnetic field of H = 527 G (FC mode: a_H—light red squares; a_L—dark red squares. ZFC mode: a_H—light olive triangles; a_L—dark olive triangles. H_2O—light blue points; Cu—dark green dot).

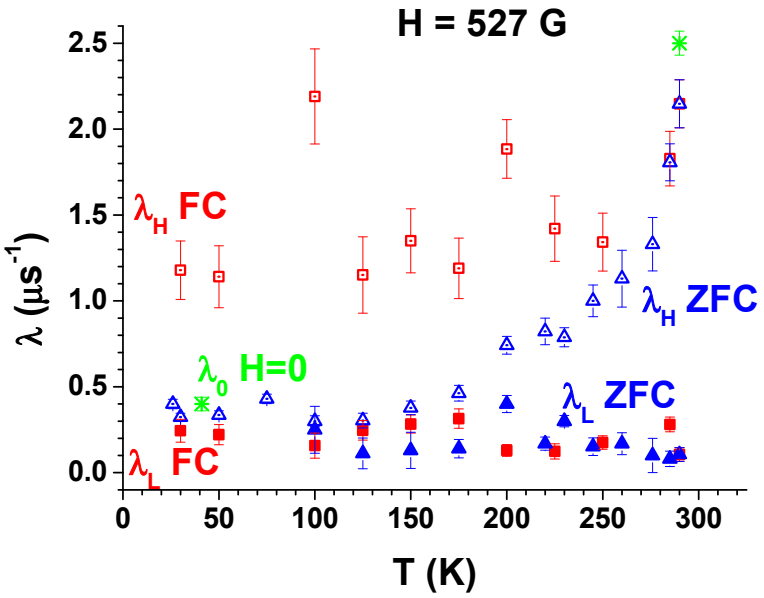

Figure 6. Temperature dependence of the relaxation rates of muon polarization, λ_H and λ_L, in a magnetic field H = 527 G (FC mode: λ_H—light red squares; λ_L—dark red squares. ZFC mode: λ_H—light blue triangles; λ_L—dark blue triangles; and λ_0 in H = 0 (green star)).

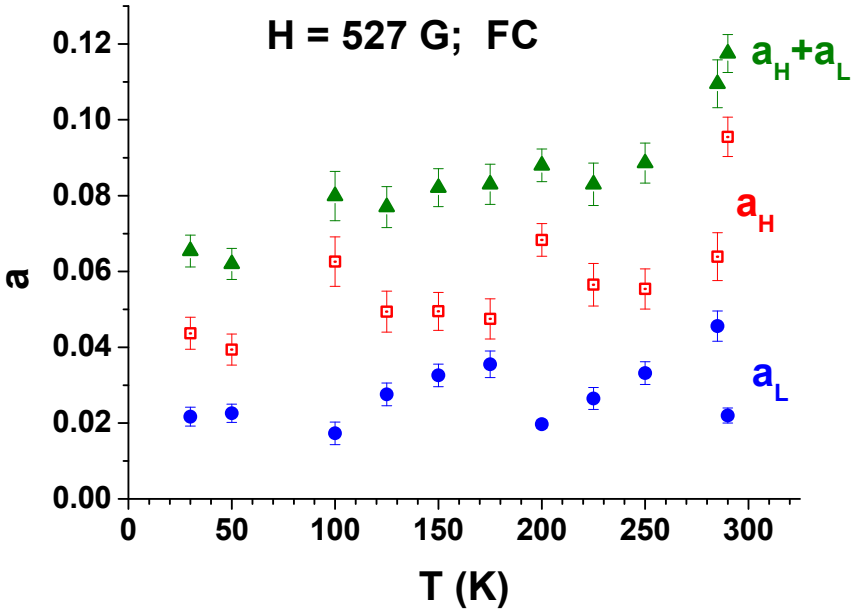

Figure 7. Temperature dependence of the populations of the upper F_H and lower F_L frequencies in a magnetic field H = 527 G in the FC mode (a_H—light red squares; a_L—dark blue dots; and $a_H + a_L$—dark olive triangles).

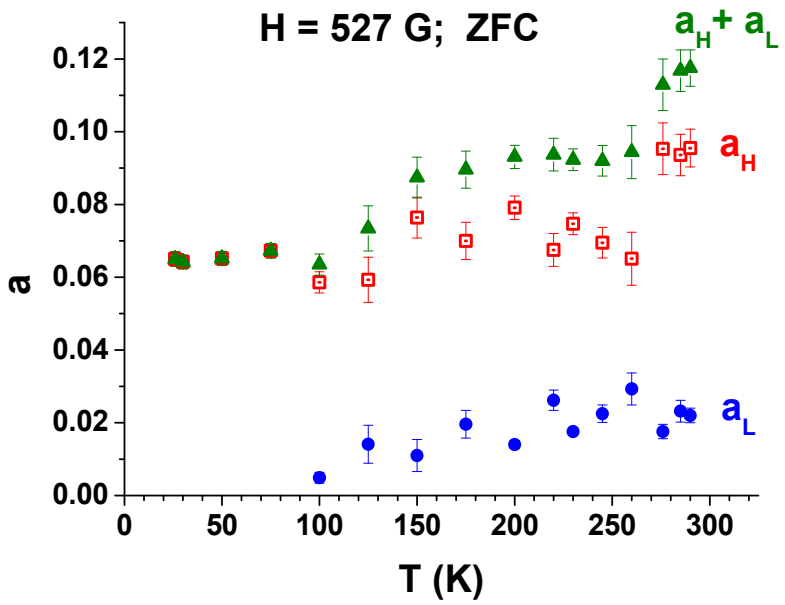

Figure 8. Temperature dependence of the populations of the upper F_H and lower F_L frequencies in a magnetic field H = 527 G in the ZFC mode (a_H—light red squares; a_L—dark blue dots; and $a_H + a_L$—dark olive triangles).

In the ZFC measurement mode, in the temperature range of 26–100 K, one precession frequency of muon spin was observed. With an increase in the sample temperature, starting from T = 100 K, two muon spin precession frequencies, F_H and F_L, appeared; moreover, the F_H frequency began to increase noticeably. For comparison, the same figure (Figure 5) shows the behavior of the precession frequency of muons in a sample of H_2O and Cu. The relationship $F_H > F_{Cu,H_2O} > F_L$ is maintained throughout the entire temperature regime.

Figure 6 shows the behavior of the parameters λ_H, λ_L, and λ_0 in the sample temperature range of 26 K to 290 K. Here, λ_0 is the relaxation rate of muon polarization in a zero external magnetic field. A noticeable difference of the parameter λ_0 at T = 290 K from the value at T = 41 K is associated with the dynamics of nanoparticles in the medium at T = 290 K. In the FC measurement mode, the values of λ_H and λ_L were practically independent within the error limits at the sample temperature. In the ZFC measurement mode in the temperature range 26–125 K, $\lambda_H \approx \lambda_0$ (Figure 6). At these temperatures, the sample behavior was paramagnetic (Figures 5 and 6). With a further increase in the temperature of the sample, the parameter λ_H began to increase noticeably, and was practically comparable with the value of λ_0 at T = 290 K.

Figures 7 and 8 display the behavior of the populations of the upper F_H and lower F_L frequencies (a_H and a_L) versus sample temperature in FC and ZFC measurements.

A significant excess of a_H over a_L was observed over the entire temperature range. This difference was especially large at room temperature, when the solution was a real ferrofluid, and not ice. Definite structures of the temperature dependence of the quantities a_H and a_L were observed in FC measurements.

The sum of the partial amplitudes at all temperature points was almost 20% less than the amplitude of the precession obtained in water (H_2O) (Figure 9). This difference can be explained by the fact that some of the muons stop in places with large inhomogeneity in the field. This leads to their rapid depolarization, and the oscillation of their spins was not observed. The behavior of positive muons in water has been well-studied previously [44]. Nevertheless, we conducted our own measurements in our cryostat for confirmation.

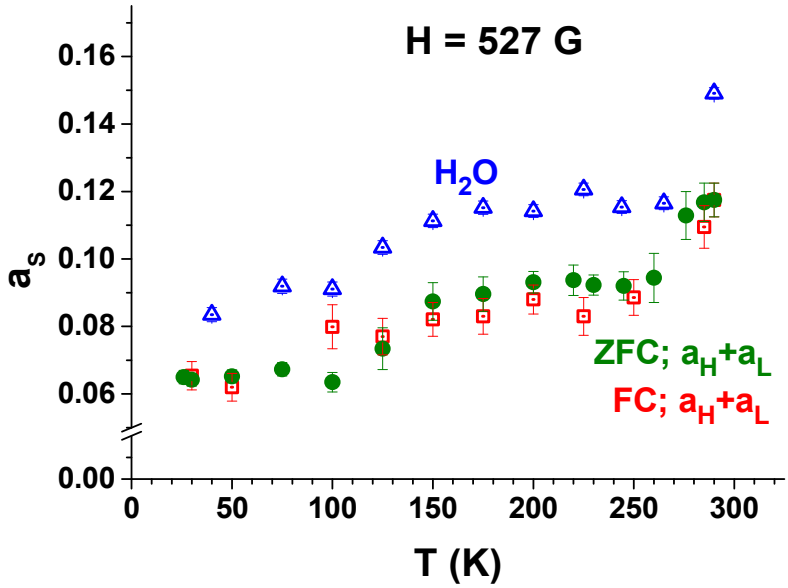

Figure 9. Temperature dependences of the fraction of the asymmetry of the muon component in a transverse magnetic field H= 527 G in the FC mode ($a_H + a_L$—open red squares), in the ZFC mode ($a_H + a_L$—dark olive points), and for the water sample (H_2O—light blue triangles).

3.4. The Estimation of the Magnitude of the Magnetic Field Near the Nanoparticle

The relaxation function $G(t)$ for the sum of spectra in the temperature range 26–100 K, obtained in the ZFC mode in an external magnetic field H = 527 G, and its satisfactory fitting curve obtained within the framework of the two-frequency hypothesis presented in Equation (3), are depicted in Figure 10.

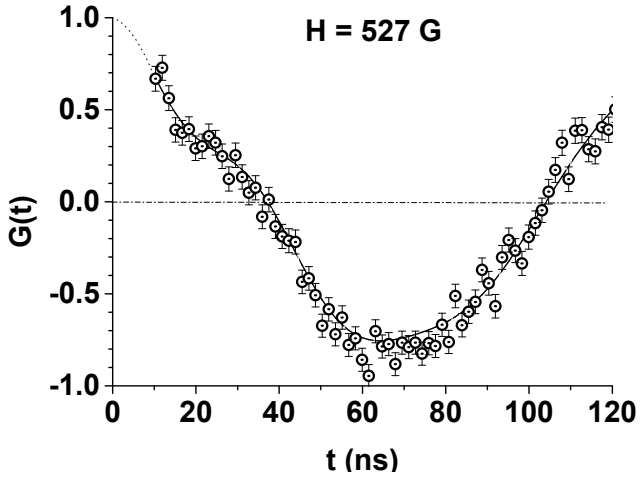

Figure 10. Function $G(t)$ in the ZFC mode in an external magnetic field H = 527 G; the spectra are added at temperatures from 26 to 100 K.

Therefore, in addition to the main contribution characterized by the amplitude $a_L = 0.099 \pm 0.001$, the relaxation rate $\lambda_L = 0.35 \pm 0.03$ μs^{-1}, and the frequency $F_L = 7.167 \pm 0.002$ MHz, corresponding to a magnetic field value of $H = 528.76 \pm 0.14$ G, a small supplementary contribution is determined with the parameters $a_H = 0.027 \pm 0.007$, $\lambda_H = 24 \pm 6$ μs^{-1}, and $F_H = 26.5 \pm 0.6$ MHz, corresponding to a magnetic field value of $H = 1.96 \pm 0.44$ kG.

This contribution is associated with the muon stopping in the immediate vicinity of nanoparticles and inside nanoparticles. Thus, direct measurement of the magnetization of the nanoscale object was carried out.

4. Conclusions

A muon spectroscopy study of a ferrofluid with a 3% volume concentration of $CoFe_2O_4$ magnetic nanoparticles dispersed in H_2O has been reported.

New information on the magnetic properties of the system have been determined or confirmed using a new method:

(i) The structure and value of the magnetization of a ferrofluid with $CoFe_2O_4$ nanoparticles depend on the viscosity of the liquid itself.
(ii) At room temperature (~290 K), when the sample was a superparamagnetic system, from the experimentally determined magnetization an average magnetic field of 20 G was obtained.
(iii) A small fraction of the sample with negative magnetization, characteristic for diamagnetic systems, was also determined.
(iv) At low temperatures (~30 K), the sample exhibits paramagnetic behavior in a magnetic field.
(v) The magnetic field inside and in the immediate vicinity of the $CoFe_2O_4$ nanoparticles was first measured by the μSR method, and its value was B = 1.96 ± 0.44 kG.

Although the presented results belong primarily to the category of fundamental knowledge, with the development of technologies for nanoparticle manipulation in technical and bio-medical applications, such information may turn out to be valuable.

Author Contributions: Conceptualization, validation, formal analysis, investigation, resources, writing—original draft, S.I.V.; conceptualization, validation, formal analysis, investigation, resources, writing—original draft, M.B.; conceptualization, validation, formal analysis, investigation, resources, writing—original draft, D.B.; conceptualization, validation, formal analysis, investigation, resources, writing—original draft, V.N.D.; conceptualization, validation, formal analysis, investigation, writing—original draft, A.L.G.; conceptualization, validation, formal analysis, investigation, resources, writing—original draft, K.I.G.; conceptualization, validation, formal analysis, investigation, writing—original draft, E.N.K.; conceptualization, validation, formal analysis, investigation, S.A.K.; conceptualization, validation, formal analysis, investigation, resources, writing—original draft, C.S.; and conceptualization, validation, formal analysis, investigation, writing—original draft, G.V.S. All authors have read and agreed to the published version of the manuscript.

Funding: This work was partially accomplished with financial support from the RO-JINR Projects Nos.268/21.05.2020 items 8 and 77, 269/21.05.2020 items 11 and 80, and 366/11.05.2021 item 17, 365/11.05.2021 item 18.

Institutional Review Board Statement: Not applicable.

Informed Consent Statement: Not applicable.

Data Availability Statement: Data supporting the reported results are available at the request of the appropriate author. The data are not available to the public due to corporate rules.

Acknowledgments: The authors are grateful to Sergei Lysenko (ITCh, Perm) for preparation of the ferrofluid and to the staff of the accelerator department of the NRC "Kurchatov Institute", PNPI for the high quality of technical support during research. Vorob'ev S.I. is grateful to the Governor of the Leningrad Region for supporting the work with the nominal scientific scholarship of the Governor of the Leningrad Region in the category "leading scientists".

Conflicts of Interest: The authors declare no conflict of interest. The funders had no role in the design of the study; in the collection, analyses, or interpretation of data; in the writing of the manuscript; or in the decision to publish the results.

References

1. Gubin, S.P.; Koksharov, Y.A.; Khomutov, G.B.; Yurkov, G.Y. Magnetic nanoparticles: Preparation, structure and properties. *Russ. Chem. Rev.* **2005**, *74*, 489–520. [CrossRef]
2. Joseph, S.A.; Mathew, S. Ferrofluids: Synthetic Strategies, Stabilization, Physicochemical Features, Characterization, and Applications. *ChemPlusChem* **2014**, *79*, 13821420.
3. Torres-Diaz, I.; Rinaldi, C. Recent progress in ferrofluids research: Novel applications of magnetically controllable and tunable fluids. *Soft Matter* **2014**, *10*, 8584–8602. [CrossRef]

4. Vestal, C.R.; Zhang, Z.J. Magnetic spinel ferrite nanoparticles from microemulsions. *Int. J. Nanotechnol.* **2004**, *1*, 240–263. [CrossRef]
5. Odenbach, S. (Ed.) *Colloidal Magnetic Fluids: Basics, Development and Application of Ferrofluids*; Springer: Berlin/Heidelberg, Germany, 2009; p. 763.
6. Socoliuc, V.; Peddis, D.; Petrenko, V.I.; Avdeev, M.V.; Susan-Resiga, D.; Szabó, T.; Turcu, R.; Tombácz, E.; Vékás, L. Magnetic Nanoparticle Systems for Nanomedicine—A Materials Science Perspective. *Magnetochemistry* **2019**, *6*, 2. [CrossRef]
7. Popescu, R.C.; Andronescu, E.; Vasile, B.S. Recent Advances in Magnetite Nanoparticle Functionalization for Nanomedicine. *Nanomaterials* **2019**, *9*, 1791. [CrossRef] [PubMed]
8. Hosu, O.; Tertis, M.; Cristea, C. Implication of Magnetic Nanoparticles in Cancer Detection, Screening and Treatment. *Magnetochemistry* **2019**, *5*, 55. [CrossRef]
9. Bilal, M.; Mehmood, S.; Rasheed, T.; Iqbal, H.M.N. Bio-Catalysis and Biomedical Perspectives of Magnetic Nanoparticles as Versatile Carriers. *Magnetochemistry* **2019**, *5*, 42. [CrossRef]
10. Katz, E. Magnetic Nanoparticles. *Magnetochemistry* **2020**, *6*, 6. [CrossRef]
11. Larkin, T.I.; Bol'ginov, V.V.; Stolyarov, V.S.; Ryazanov, V.V.; Vernik, I.V.; Tolpygo, S.K.; Mukhanov, O.A. Ferromagnetic Josephson switching device with high characteristic voltage. *Appl. Phys. Lett.* **2012**, *100*, 222601. [CrossRef]
12. Bergeret, F.S.; Verso, A.; Volkov, A.F. Electronic transport through ferromagnetic and superconducting junctions with spin-filter tunneling barriers. *Phys. Rev. B* **2012**, *86*, 214516. [CrossRef]
13. Richardson, C.L.; Devine-Stoneman, J.M.; Divitini, G.; Vickers, M.E.; Chang, C.-Z.; Amado, M.; Moodera, J.S.; Robinson, J.W.A. Structural properties of thin-film ferromagnetic topological insulators. *Sci. Rep.* **2017**, *7*, 12061. [CrossRef]
14. Parlato, L.; Caruso, R.; Vettoliere, A.; Satariano, R.; Ahmad, H.G.; Miano, A.; Montemurro, D.; Salvoni, D.; Ausanio, G.; Tafuri, F.; et al. Characterization of scalable Josephson memory element containing a strong ferromagnet. *J. Appl. Phys.* **2020**, *127*, 193901. [CrossRef]
15. Felicia, L.J.; Vinod, S.; Philip, J. Recent Advances in Magnetorheology of Ferrofluids (Magnetic Nanofluids)—A Critical Review. *J. Nanofluids* **2016**, *5*, 1–22. [CrossRef]
16. Kole, M.; Khandekar, S. Engineering applications of ferrofluids: A review. *J. Magn. Magn. Mater.* **2021**, *537*, 168222. [CrossRef]
17. Krasia-Christoforou, T.; Socoliuc, V.; Knudsen, K.D.; Tombácz, E.; Turcu, R.; Vékás, L. From Single-Core Nanoparticles in Ferrofluids to Multi-Core Magnetic Nanocomposites: Assembly Strategies, Structure, and Magnetic Behavior. *Nanomaterials* **2020**, *10*, 2178. [CrossRef] [PubMed]
18. Lysenko, S.N.; Lebedev, A.V.; Astaf'eva, S.A.; Yakusheva, D.E.; Balasoiu, M.; Kuklin, A.I.; Kovalev, Y.S.; Turchenko, V.A. Preparation and magneto-optical behavior of ferrofluids with anisometric particles. *Phys. Scr.* **2020**, *95*, 044007. [CrossRef]
19. Bica, D.; Vekas, L.; Avdeev, M.V.; Marinica, O.; Socoliuc, V.; Balasoiu, M.; Garamus, V.M. Sterically stabilized water based magnetic fluids: Synthesis, structure and properties. *J. Magn. Magn. Mater.* **2007**, *311*, 17–21. [CrossRef]
20. Lebedev, A.V.; Lysenko, S.N. A multifunctional stabilizer of magnetic fluids. *Appl. Phys. Lett.* **2009**, *95*, 013508. [CrossRef]
21. Lysenko, S.N.; Yakushev, R.M.; Strel'nikov, V.N.; Gabdrakhimova, Y.I.; Borisova, I.A. Steric stabilization and functionalization of magnetite particles and preparation of colloid magnetite dispersions in oligomeric media. *Russ. J. Appl. Chem.* **2010**, *83*, 1399–1402. [CrossRef]
22. Vekas, L.; Rasa, M.; Bica, D. Physical properties of magnetic fluids and nanoparticles from magnetic and magneto-rheological measurements. *J. Colloid Interface Sci.* **2000**, *231*, 247–254. [CrossRef]
23. Socoliuc, V.; Bica, D.; Vekas, L. Estimation of magnetic particle clustering in magnetic fluids from static magnetization experiments. *J. Colloid Interface Sci.* **2003**, *264*, 141–147. [CrossRef]
24. Lebedev, A.V. Temperature dependence of magnetic moments of nnoparticles and their dipole interaction in magnetic fluids. *J. Magn. Magn. Mater.* **2015**, *374*, 120–124. [CrossRef]
25. Sergeenkov, S.; Stan, C.; Cristescu, C.P.; Balasoiu, M.; Perov, N.S.; Furtado, C. Evidence forfield induced proximity type behavior in based ferromagnetic nanofluid. *Philos. Mag. Lett.* **2017**, *97*, 287–293. [CrossRef]
26. Gamarra, L.F.; Pontuschka, W.M.; Mamani, J.B.; Cornejo, D.R.; Oliveira, T.R.; Vieira, E.D.; Costa-Filho, A.J.; Amaro, E., Jr. Magnetic characterization by SQUID and FMR of a biocompatible ferrofluid based on Fe_3O_4. *J. Phys. Condens. Matter* **2009**, *21*, 115104. [CrossRef]
27. Granata, C.; Vettoliere, A. Nano superconducting quantum interface device: A powerful tool for nanoscale investigations. *Phys. Rep.* **2016**, *614*, 1–69. [CrossRef]
28. Kuncser, V.; Schinteie, G.; Sahoo, B.; Keune, W.; Bica, D.; Vekas, L.; Filoti, G. Magnetic interactions in water based ferrofluids studied by Mössbauer spectroscopy. *J. Phys. Condens. Matter* **2006**, *19*, 016205. [CrossRef]
29. Spanu, V.; Filoti, G.; Bica, D.; Balasoiu, M.; Crisan, O. Mossbauer Spectroscopy Studies of Fine Fe_3O_4 Particles Contained in Magnetic Fluids. *Rom. Rep. Phys.* **1995**, *47*, 299–307.
30. Grabcev, B.; Balasoiu, M.; Tarziu, A.; Kuklin, A.I.; Bica, D. Application of contrast variation method in SANS experiments with ferrofluids. *J. Magn. Magn. Mater.* **1999**, *201*, 140–143. [CrossRef]
31. Avdeev, M.V.; Balasoiu, M.; Aksenov, V.L.; Garamus, V.M.; Kohlbrecher, J.; Bica, D.; Vekas, L. On the magnetic structure of magnetite/oleic acid/benzene ferrofluids by small-angle neutron scattering. *J. Magn. Magn. Mater.* **2004**, *270*, 371–379. [CrossRef]
32. Balasoiu, M.; Kuklin, A.I. Magnetic scattering determination from SANS contrast variation experiments at IBR-2 reactor. *Rom. J. Phys.* **2016**, *61*, 473–482.

33. Muehlbauer, S.; Honecher, D.; Perigo, E.A.; Bergner, F.; Disch, S.; Heinemann, A.; Erokhin, S.; Berkov, D.; Leighton, C.; Eskiidsen, M.; et al. Magnetic small-angle neutron scattering. *Rev. Mod. Phys.* **2019**, *91*, 015004. [CrossRef]
34. Schenck, A. *Muon Spin Rotation Spectroscopy*; Adam Hilger, Ltd.: Bristol, UK, 1985.
35. Jackson, T.J.; Binns, C.; Forgan, E.M.; Morenzoni, E.; Niedermayer, C.; Gluckler, H.; Hofer, A.; Luetkens, H.; Prokscha, T.; Riseman, T.M.; et al. Superparamagnetic relaxation in iron nanoclusters measured by low energy muon spin rotation. *J. Phys. Condens. Matter* **2000**, *12*, 1399–1411. [CrossRef]
36. Boekema, C.; Lichti, R.L.; Brabers, V.A.M.; Denison, A.B.; Cooke, D.W.; Heffner, R.H.; Hutson, R.L.; Leon, M.; Schillaci, M.E. Magnetic interactions, bonding, and motion of positive muons in magnetite. *Phys. Rev. B* **1985**, *31*, 1233. [CrossRef] [PubMed]
37. Boekema, C.; Lichti, R.L.; Chan, K.C.B.; Brabers, V.A.M.; Denison, A.B.; Cooke, D.W.; Heffner, R.H.; Hutson, R.L.; Schillaci, M.E. Experimental evidence for a Mott-Wigner glass phase of magnetite above the Verwey temperature. *Phys. Rev. B* **1986**, *33*, 210. [CrossRef]
38. Wang, J.; Zhao, F.; Wu, W.; Cao, S.-H.; Zhao, G. Magnetic properties in silica-coated $CoFe_2O_4$ nanoparticles: Quantitative test for a theory of single-domain particles with cubic anisotropy. *Phys. Lett. A* **2012**, *376*, 547–549. [CrossRef]
39. Balasoiu, M.; Barsov, S.G.; Bica, D.; Vekas, L.; Vorob'ev, S.I.; Gritsaj, K.I.; Duginov, V.N.; Zhukov, V.A.; Komarov, E.N.; Koptev, V.P.; et al. muSR Study of the Properties of Fe_3O_4-Based Nanostructured Magnetic Systems. *JETP Lett.* **2008**, *88*, 210–213. [CrossRef]
40. Lebedev, A.V.; Lysenko, S.N. Magnetic fluids stabilized by polypropylene glycol. *J. Magn. Magn. Mater.* **2011**, *323*, 1198–1202. [CrossRef]
41. Yakushev, R.M.; Lysenko, S.N.; Tiunova, T.G.; Borisova, I.A.; Lebedev, A.V. Rheology of magnetite dispersions in oligo(propylene glycol) and the structure of the stabilizing layer on dispersed phase particles. *Colloid J.* **2013**, *75*, 226–230. [CrossRef]
42. Barsov, S.G.; Vorob'ev, S.I.; Koptev, V.P.; Kotov, S.A.; Mikirtych'yants, S.M.; Shcherbakov, G.V. The μSR setup on the muon beam of the synchrocyclotron at the Konstantinov Institute of Nuclear Physics. *Instrum. Exp. Tech.* **2007**, *50*, 750–756. [CrossRef]
43. Smilga, V.P.; Belousov, Y.M. *The Muon Method in Science*; Nova Science Publishers: New York, NY, USA, 1992.
44. Percival, P.W. Muonium formation in water and aqueous solutions. *Hyperfine Interact.* **1981**, *8*, 315–324. [CrossRef]